Hindawi
Advances in Civil Engineering
Volume 2019, Article ID 8914708, 11 pages
https://doi.org/10.1155/2019/8914708

Research Article

Prediction of Response of Existing Building Piles to Adjacent Deep Excavation in Soft Clay

Yao-Ying Liang,[1] Nian-Wu Liu ,[1] Feng Yu,[1] Xiao-Nan Gong,[2] and Yi-Tian Chen[1]

[1]*Institute of Foundation and Structure Technologies, Zhejiang Sci-Tech University, Hangzhou 310018, China*
[2]*Research Center of Coastal and Urban Geotechnical Engineering, Zhejiang University, Hangzhou 310058, China*

Correspondence should be addressed to Nian-Wu Liu; zjulnw@163.com

Received 8 August 2019; Accepted 4 November 2019; Published 5 December 2019

Academic Editor: Pier Paolo Rossi

This study investigates building settlements near excavations in soft clay. A simplified theoretical method is proposed to predict the additional settlements and axial forces of excavation-adjacent existing building floating piles in soft clay. The soil displacement is simplified as a line or broken line along the depth direction, depending on the distance from the excavation. A hyperbolic model is applied to calculate the skin friction and tip resistance induced by the vertical soil displacement. The parameters of the hyperbolic model are corrected to fit data from in-service piles. Based on the load-transfer curve method, the additional settlements and axial forces are determined. The measured data of 17 floating piles from two excavation cases in Hangzhou, China, show good agreement with the calculated values. The results show that the position of the neutral point of the loaded pile varies with the soil settlement. Because of the upper structure, the theoretical settlements for piles near the excavation are larger than those obtained from the measured values; for distant piles, this relationship is reversed. The proposed prediction methodology is expected to guide the design of practical excavations.

1. Introduction

Excavations in urban spaces are gradually increasing in order to utilize the underground space for transportation infrastructure, underground shopping malls, and other engineering works. The areas of excavation have exceeded 50000 m^2, and the maximum depths of these projects have exceeded 30 m; namely, the excavations have become larger, deeper, and more crowded. Instances of deformation and even damage to adjacent buildings by excavation projects are also increasing. During excavation, unloading and precipitation inevitably induce stress and displacement fields in the adjacent soil; these displacement fields cause corresponding additional deformation and forces in the existing piles (Figure 1). Several methods to estimate excavation-induced soil displacements have been proposed, including empirical methods [1–5] and numerical simulation [6–8]. The displacement-induced skin friction and tip resistance to existing piles located near the excavation area are always calculated using hyperbolic models [9–13] or nonlinear models [14–17]. Multiple new methodologies have been proposed to estimate or predict the responses of existing piles to new excavations via theoretical and numerical simulations [18–23].

This paper presents a methodology to predict the responses of existing floating piles to adjacent deep excavation in soft clay. The main achievements of the study are as follows: (1) a simplified model of excavation-induced soil displacement fields was established based on previous research and numerical simulation; (2) the parameters of the hyperbolic model were corrected to suit the existing piles; and (3) the additional settlements and axial forces were obtained using the load-transfer method. The proposed methodology was verified using data from two engineering cases, in which the deformations of the adjacent floating piles were caused by deep excavations for metro stations.

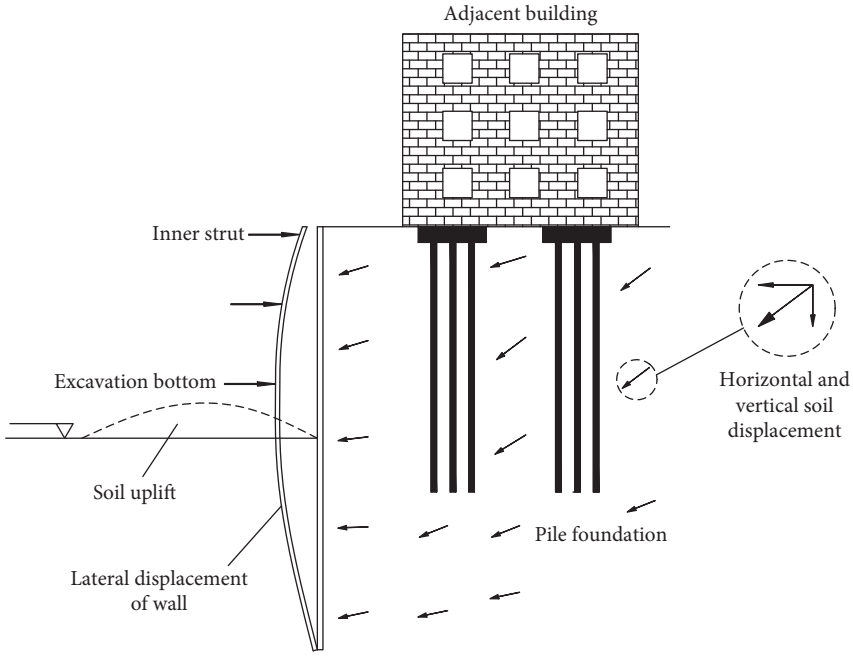

Figure 1: Displacement field around existing pile induced by excavation.

2. Regular Deep Soil Settlement near Excavation

The estimation of the soil displacement field induced by deep excavation is complex. Such displacement is always influenced by multiple factors, including the excavation depth, descending of groundwater, characteristics of the support system, and parameters of the soil layers. The apparent influence range (AIR) is necessary to estimate the soil displacement. In all previous studies on this topic, the displacement field has been divided into two or three [24–26]. Upon analyzing a large volume of engineering case data, Ou et al. [24] proposed that surface subsidence can occur over an area exceeding five times the excavation depth and defined the AIR. Hsieh and Ou [25] further proposed that the primary and secondary influence range is $2H_e$ (where H_e is the depth of the excavation). Caspe [26] described the boundary of the AIR as a helical line.

For a detailed analysis of soil displacement, the characteristics of the excavation system should be considered; the finite element method is adopted to verify the average soil settlements in soft clay induced by excavation with inner struts [27]. The simulated excavation depth is 20 m, and four inner struts are adopted. The depths of the supports are −1 m, −6 m, −11 m, and −16 m. Based on the soil in Hangzhou, China, the values of the finite element model parameters are shown in Table 1. The values of the deep soil settlements calculated using the finite element method are shown in Figure 2.

The simulated results show that, in the horizontal range 0–$1.0H_e$, the soil settlement first remains constant and then linearly decreases along the depth and, in the range 1–$2.0H_e$, the settlement linearly decreases. In this study, by simplifying the spiral boundary model proposed by Caspe [26], a model of the soil settlement is proposed based on the simulated results, as shown in Figure 3. In the horizontal range 0–$1.0H_e$ (area *I*), the settlement is considered to remain constant at depths from 0 to $0.5H_e$ and to decrease linearly at depths $>0.5H_e$. In area II, i.e., the horizontal range 1.0–$2.0H_e$, the soil settlement decreases linearly. An equation to calculate the soil settlement as a function of depth can be obtained according to the geometric relationship.

When $x < 1.0H_e$,

$$\begin{cases} \delta_{vz,x} = \delta_{v0,x}, & z < 0.5H_e, \\ \delta_{vz,x} = \dfrac{2H_e\delta_{v0,x}}{w} z - \dfrac{\left(2H_e^2 + 2H_eD - Dx\right)\delta_{v0,x}}{w}, & 0.5H_e < z < \dfrac{-D}{H_e} + H_e + D. \end{cases} \tag{1}$$

When $1.0H_e < x < 2.0H_e$,

$$\delta_{vz,x} = \frac{2H_e\delta_{v0,x}}{w} z + \delta_{v0,x}, \tag{2}$$

where $w = Dx - 2H_eD - H_e^2$, $\delta_{vz,x}$ is the soil settlement value at the depth z and lateral distance x from the retaining structure, $\delta_{v0,x}$ is the soil settlement value of the surface soil

Table 1: Input parameters of the finite element method.

Name of soil layer	Thickness (m)	γ_{sat} (kN/m^3)	c (kPa)	φ (°)	E_{50}^{ref} (kN/m^2)	E_{oed}^{ref} (kN/m^2)	E_{ur}^{ref} (kN/m^2)	G_0^{ref} (kN/m^2)	$\gamma_{0.7}$
Silty clay	6	17	18	15	5000	5000	1.9×10^4	1.1×10^5	2×10^{-3}
Soft clay	29	16	16	18	3000	3000	1.8×10^4	6×10^4	2×10^{-3}
Medium clay	30	18	50	30	8000	8000	2.7×10^4	5×10^5	2×10^{-3}

γ_{sat} = effective saturated unit weight; c and φ = cohesion and friction angle of soil, respectively; E_{50}^{ref} = secant stiffness in the standard drained triaxial test; E_{oed}^{ref} = tangent stiffness for primary oedometer loading; E_{ur}^{ref} = unloading-reloading stiffness; G_0^{ref} and $\gamma_{0.7}$ are the parameters related to small strain behaviors.

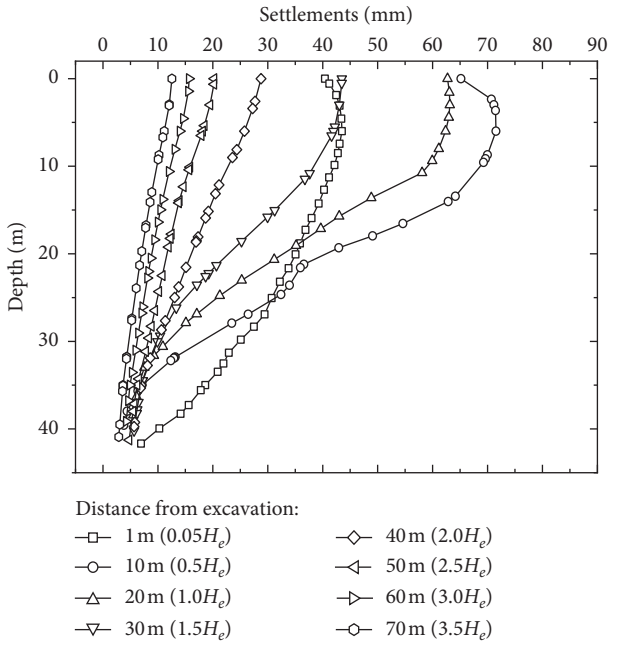

Figure 2: Regular deep soil settlement at different distances from excavation.

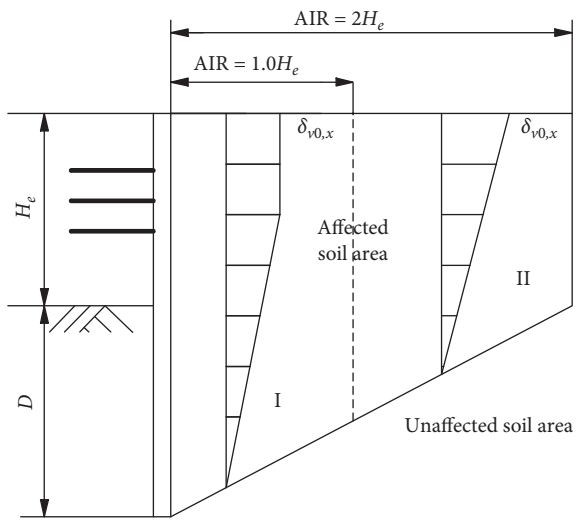

Figure 3: Apparent influence range (AIR) and regions of vertical soil displacement changes.

at distance x from the retaining structure, H_e is the depth of the excavation, and D is the depth of the underground concrete diaphragm wall.

3. Relationship between Skin Friction of In-Service Piles and Relative Pile-Soil Displacement

In this study, the hyperbolic model is adopted to calculate the skin friction of in-service piles with corrected parameters. The original points and asymptotic values of the hyperbolic model differed for the piles that were already in service before the excavation.

3.1. Negative Friction Model. A modified hyperbolic model, as shown in Figure 4, can be used to evaluate the relationship between the unit negative friction and soil-pile relative settlements. Gómez et al. [28] have proposed that, during the unloading process, the unloading stiffness is equal to the initial stiffness. Therefore, the skin friction model during unloading can also be expressed as a hyperbolic model. For piles with top structures, the skin friction is exerted to a certain extent. In the process of pile design, the technical code for building pile foundations [29] stipulates a safety factor of 2; in other words, the bearing capacity of the pile is one-half of the limiting value for that when the pile is in service. Furthermore, Geddes [30] proposed that the skin friction presents a triangular distribution along the depth. We can therefore hypothesize that the shear stress and end resistance are exerted to half of the ultimate shear stress; therefore, the original point (shear stress/ultimate shear stress) of the hyperbolic model is 0.5. Then, referring to the pile uplift coefficient, the ratio of the negative frictional resistance to the ultimate positive frictional resistance is considered to be approximately 0.7 [29]. The limiting value of the ratio of shear stress to ultimate shear stress is therefore approximately −0.7 for negative friction. This model can be used to calculate the negative friction induced by excavation in soft clay.

The mathematical expression for the model is as follows:

$$\tau_s(z) = \frac{S_{rs}(z)}{a_r + b_r S_{rs}(z)}, \tag{3}$$

where $\tau_s(z)$ is the negative friction at depth z, $S_{rs}(z)$ is the relative displacement of the pile and soil at depth z, and a_r and b_r are the empirical parameters determined experimentally or from test results.

The traditional method used to evaluate a_r and b_r, developed by Lee and Xiao [31], is complex and relies on measured values. Zhang et al. [13] proposed a simplified approach to calculate these two parameters; the approach is tailored to fit the modified hyperbolic model in this study.

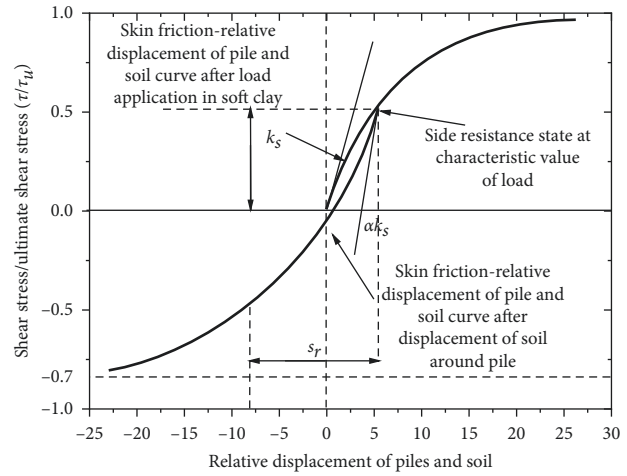

Figure 4: Calculation model of negative lateral resistance and relative displacement of pile and soil.

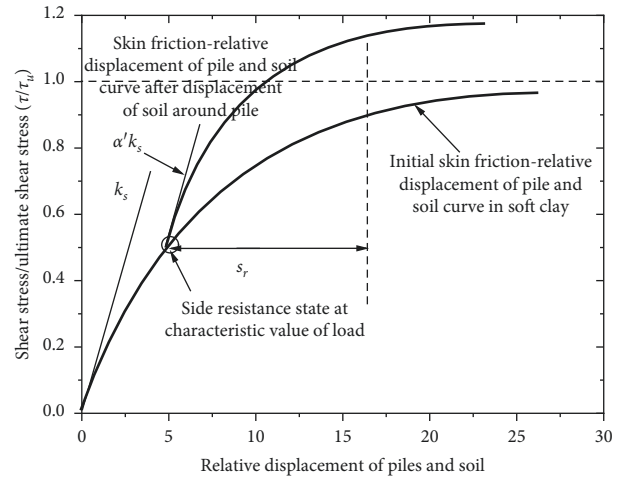

Figure 5: Calculation model of positive lateral resistance and relative displacement of pile and soil.

According to the simplified method, a_r can be calculated with reference to the research results of Randolph and Wroth [32] which is based on the Winkler model of the soil, and the empirical calculation formula that adds the coefficient α to account for the change in the original point is as follows:

$$a_r = \frac{1}{\alpha k_s} = \frac{r_0}{\alpha G_s} \ln\left(\frac{r_m}{r_0}\right), \tag{4}$$

where r_0 is the pile radius, G_s is the soil shear modulus, α is a coefficient related to the slope of the hyperbolic original point that can be obtained from the geometric relationship in Figure 4, and r_m is the radial distance from the pile axes to a point where the stress induced by the pile is negligible, which can be estimated as suggested by Zhang et al. [13].

The value of $1/b_r$ is the asymptote value of the hyperbola; b_r can be calculated as follows [13]:

$$b_r = \frac{1}{\beta \tau_{su}} = \frac{R_{sf}}{\beta \tau_f}, \tag{5}$$

$$\tau_f = K_h \sigma_v' \tan\delta, \tag{6}$$

where σ_v' is the effective stress at a certain depth, K_h is the horizontal soil pressure coefficient, β is a coefficient determined from the asymptote of the hyperbolic model that can be obtained using geometric relations, and δ is the friction angle of the pile-soil interface. The friction angle is not easy to obtain, but it is related to the internal friction angle φ of the soil near the pile. R_{sf} is the failure ratio with a value of 0.80–0.95.

3.2. Positive Friction Model. The modified hyperbolic model shown in Figure 5 can be used to evaluate the relationship between the unit positive friction and the soil-pile relative settlements. Zhang et al. [33] proposed that the measured skin friction for piles under compression was 6% to 42% higher than the values estimated from cone penetration tests (CPTs). Therefore, it is hypothesized that the shear stresses are increased by 20% for the in-service piles. For the positive friction, the asymptotic value of the modified hyperbolic model thus approaches 1.2.

The mathematical expression for the model is as follows:

$$\tau_s(z) = \frac{S_{rs}(z)}{a_r' + b_r' S_{rs}(z)}, \tag{7}$$

where $a_r' = 1/\alpha' k_s$ and $b_r' = 1/\beta' \tau_{su}$. The values of each coefficient can be obtained from the above relations.

4. Relationship between End Resistance of In-Service Piles and Pile End Displacement

As in the positive friction model, the end resistance can be increased by 20% because of the compression effect of soil. The modified hyperbolic model is shown in Figure 6.

The mathematical expression is as follows:

$$\tau_b = \frac{S_b}{f_r + g_r S_b}, \tag{8}$$

where τ_b is the end resistance, S_b is the displacement of the pile end, and f_r and g_r are the empirical parameters.

Referring to the method proposed by Zhang et al. [34], the values of f_r and g_r can be evaluated using the following equations:

$$f_r = \frac{1}{\gamma k_b} = \frac{\pi r_0 (1 - \upsilon_b)}{4 \gamma G_b}, \tag{9}$$

$$g_r = \frac{1}{\lambda \tau_{bu}} = \frac{R_{bf}}{\lambda \tau_{bf}}, \tag{10}$$

where γ and λ are the coefficients similar to α and β above, G_b is the soil shear modulus at the pile end, ν_b is Poisson's ratio of soil at the pile end, and R_{sb} is a parameter with a value between 0.8 and 0.95.

The ultimate bearing capacity of the pile end soil can be calculated from the following formula [34]:

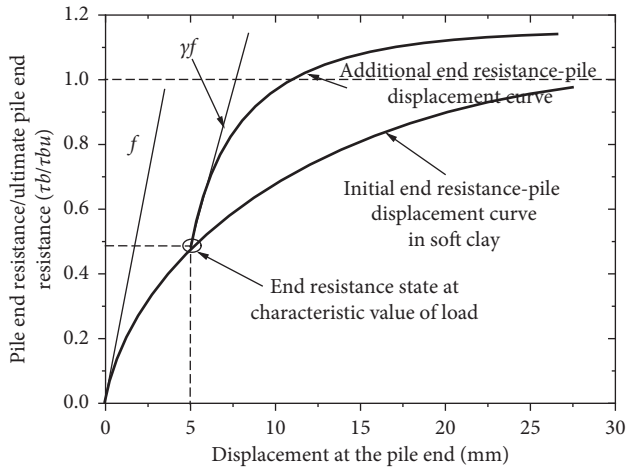

Figure 6: Calculation model of end resistance and displacement of pile.

$$\tau_{bf} = N_q \sigma'_{vb}, \tag{11}$$

where N_q is a parameter related to the internal friction angle of the soil (Berezantzev et al. [35] provided this value) and σ'_{vb} is the effective stress of the soil at the end of the pile.

5. Calculation of Additional Loading and Settlement of In-Service Pile Based on Load-Transfer Method

Adjacent piles are affected by excavation, and the effects are mainly expressed as the relative displacements of the pile and soil. The relative displacements of the pile and soil reduce the bearing capacities of the piles and induce settlement, which is the major reason for building deformation and damage. In this study, the load-transfer method is used to evaluate the attachment loading and settlement with the modified hyperbolic model proposed above.

5.1. Hypotheses

(1) The skin friction and end resistance of the existing piles are exerted to 50% of the limiting value [29]

(2) The asymptotic values of the skin friction and end resistance of existing piles are increased to 120%

(3) The relative displacement is the difference between the soil displacement and pile end displacement

(4) The compression of the pile is negligible

5.2. Calculation Process Based on Load-Transfer Method. The settlement of the shallow soil exceeds that of the pile; therefore, negative friction is generated in the downward direction. As the soil displacement gradually decreases, the pile displacement in the deep soil becomes larger than that of the soil and positive friction is generated in the upward direction. In the calculation, the pile is divided into a plurality of micro-segments, and the relative displacements of piles and soils at the end of each section are calculated to further obtain the skin friction and end resistance. The additional positive skin friction, negative skin friction, and end resistance eventually reach equilibrium, and the pile safety factor decreases. The specific steps are described below. The relative displacement, negative and positive friction, and axial force are shown in Figure 7.

Calculation steps are as follows:

(1) Pile is divided into m parts, as shown in Figure 8.

(2) Soil displacement is calculated at the end of each section according to equations (1) and (2).

(3) Pile displacement is denoted by S_{bm}, and the pile settlement curve is assumed as a straight line. The neutral point position is obtained by combining the soil settlement equations and pile settlement curve.

(4) The negative frictional resistance above the neutral point is calculated according to equation (3); the positive frictional resistance below the neutral point is calculated according to equation (7).

(5) The pile end resistance is calculated according to equation (8).

(6) The positive friction, negative friction, and end load are verified to form a balanced system:

$$f(S_{bm}) = -\left(\Gamma_{s1} + \Gamma_{s2} + \cdots + \Gamma_{sj}\right)ul + \left(\Gamma_{s,j+1} + \cdots + \Gamma_{sm}\right)ul + P_{mb}A = 0. \tag{12}$$

If equation (12) is satisfied, S_{bm} is the theoretical value of the pile settlement. If equation (12) is not satisfied, the second step is iterated until equation (12) is satisfied. The above steps can be implemented using the C coding language.

(7) The additional axial force of the pile is calculated. Above the neutral point, $P_{bk} = P_{b(k-1)} + 2\pi r l_k \tau_k$. Below the neutral point, $P_{bi} = P_{b(i-1)} - 2\pi r l_i \tau_i$. Therefore, we can obtain the additional axial force at the end of each segment to determine the additional axial force curve. This step can also be implemented using the C coding language.

6. Comparison of Theoretical and Measured Settlements

6.1. Case 1: Fengqi Road Subway Station. The Fengqi subway station is located in Hangzhou, China. This station was constructed using the cis-form method. The excavation covers a planning area of approximately 3045 m^2 with a width of 22.1 m and a length of 137.8 m. The average depth in a standard section is 24.78 m. A reinforced concrete diaphragm wall with eight inner struts (the first and the fifth are reinforced concrete struts; the remainder are steel) is used as the retaining system. The same reinforced concrete diaphragm wall, measuring 1 m in thickness and 41.88 m in depth, is also used as a water curtain and the external wall of the underground structure during station operation. Many buildings are located near the project;

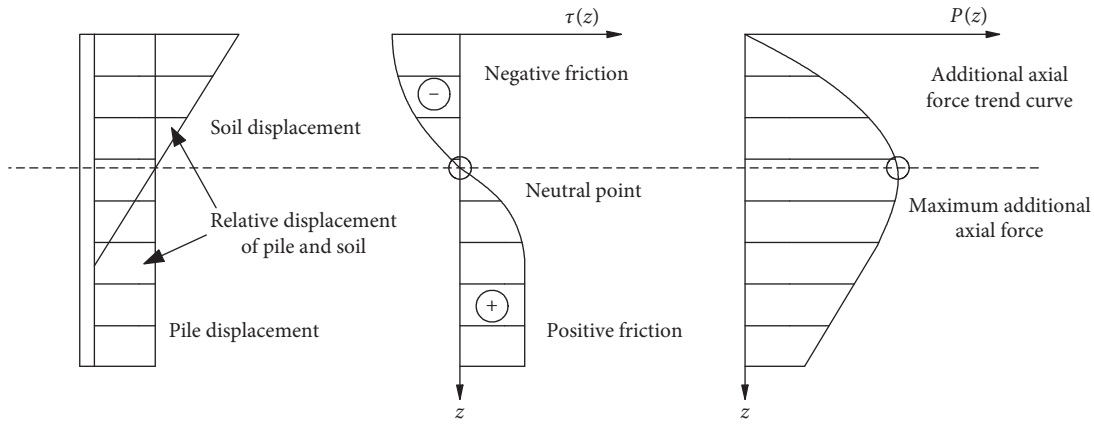

Figure 7: Diagrams of relative displacement, negative and positive friction, and axial force.

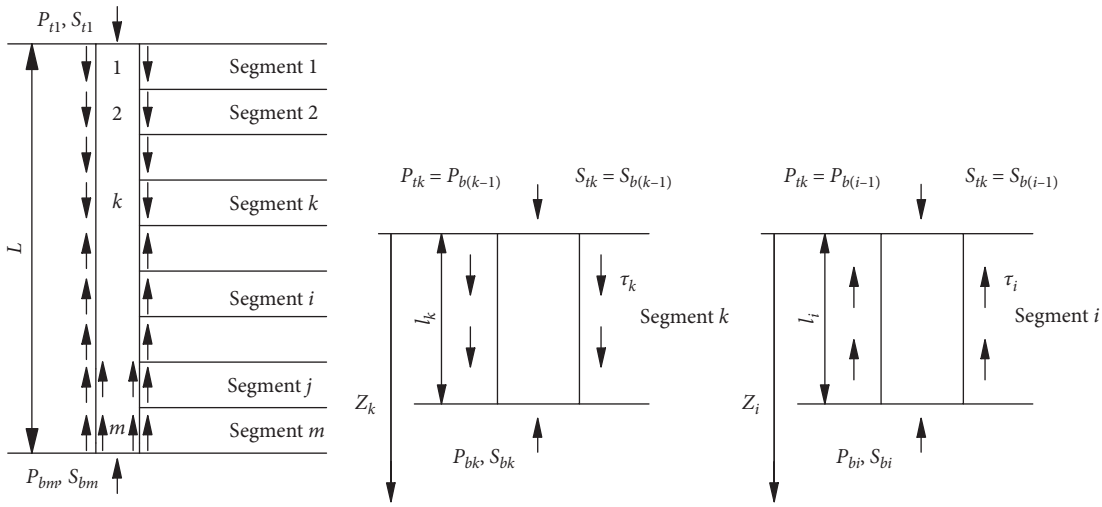

Figure 8: Schematic of force on pile unit.

most of these are located within the critical "zone of influence" of the excavation, i.e., located $<2H_e$ from the adjacent excavation.

The settlements of building *L*, with 24 m floating piles, are analyzed here because it is near the excavation, with the shortest clear distance of 3.75 m. The relative positions of the buildings and the excavation are shown in Figure 9. The soil profiles relating to the observed case and the necessary parameters for the hyperbolic model are shown in Table 2; the soil surface settlements of the measured points are shown in Table 3.

The results are shown in Figures 10–12.

6.2. Case 2: Wulin Road Subway Station. The Wulin subway station is also located in Hangzhou, China. The excavation covers a planning area of approximately 4127 m^2, measuring 21.7 m in width and 190.2 m in length. The average depth in a standard section is 18 m. Like the Fengqi Road excavation, a reinforced concrete diaphragm wall with five inner struts (one of the reinforced concrete and the remainder of steel) is used as a retaining system. The diaphragm wall extends from the ground surface to a depth of 35 m. The building K with 34 m floating piles is analyzed here. Its shortest clear distance to the excavation is 23 m. The relative positions of the buildings and the excavation are shown in Figure 13. The soil profiles and parameters are shown in Table 4, and the soil surface settlements at the measuring points are shown in Table 5.

The results are shown in Figures 14–16.

6.3. Analysis of Results. For most of the cases, the difference between the theoretical and measured values of the settlement does not exceed 20%. The comparisons indicate that the calculated values are in good agreement with the measurement results and that the calculation method is reliable. In the case of Fengqi Road, the theoretically calculated overall trend of the pile settlement at points near the excavation (M6–M10) is larger than that obtained from the measured values, but the theoretical values for the farther points (M11–M16) are smaller than the measured

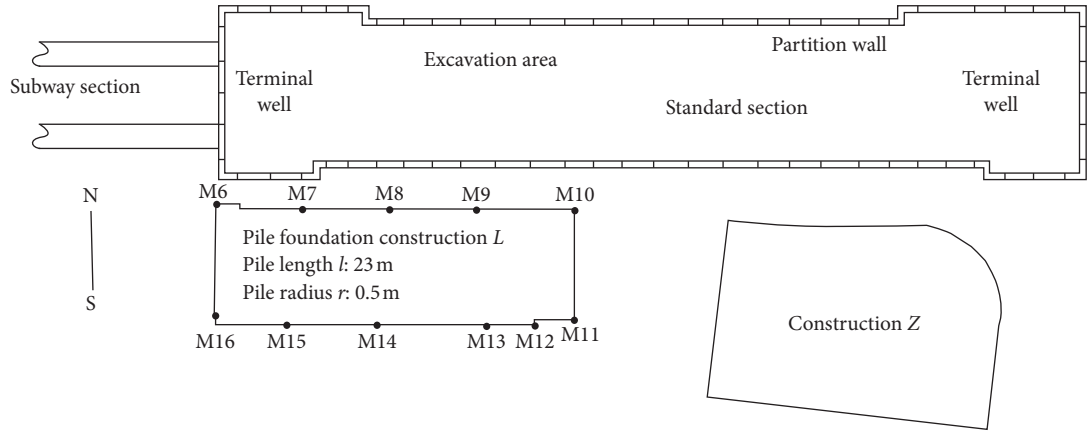

Figure 9: Plan of Fengqi Road metro station and measurement points in adjacent buildings. M6–M16 are the pile numbers.

Table 2: Soil profiles and parameters of Fengqi Road excavation.

Layer number	Name of soil layer	h (m)	c (kPa)	φ (°)	E_s (MPa)	G_s (MPa)	I_P	I_L	ν	r_0 (m)	r_m (m)	δ (°)	R_{sf}
1	Fill	4.5	10	12	2.66	4.09	—	—					
2	Silty clay	2	21.5	11.3	3.8	5.85	15.7	0.51					
3	Soft silty clay	7	13	9.5	2.6	4	14.1	0.97	0.3	0.5	21.23	30	0.9
4	Soft silty clay or silt	4.5	14	10	2.8	4.31	11.8	1.08					
5	Soft silty clay	4	13	9	2.1	3.23	17.1	1.00					
6	Silty clay	4.5	30	14	5.8	8.92	13.6	0.82					

h = thickness of the soil; c and φ = cohesion and friction angle of soil, respectively; E_s = compression modulus; G_s = shear modulus; I_P = liquid limit; I_L = plastic limit; ν = Poisson's ratio; r_0 = radius of pile; r_m = radial distance from the pile axes to a point where stress induced by the pile is negligible; δ = friction angle of the pile-soil interface; R_{sf} = failure ratio.

Table 3: Observed soil surface settlements at measuring points of Fengqi Road excavation.

Measuring points	M6	M7	M8	M9	M10	M11	M12	M13	M14	M15	M16
Distance from corner	0	13.17	27.05	40.81	56.54	56.31	50.09	42.4	25.05	10.82	−0.59
Observed settlement value (mm)	13.6	18.8	24.6	28.8	34	25	23.5	21.9	18.6	16.7	15.4

The southwest corner of the excavation serves as the reference point. The positive distance value indicates that the measuring point is located at the east side of the corner of excavation, and the negative value indicates that the measuring point is located at the west side of the corner of excavation. The specific layout of the measurement points is shown in Figure 9.

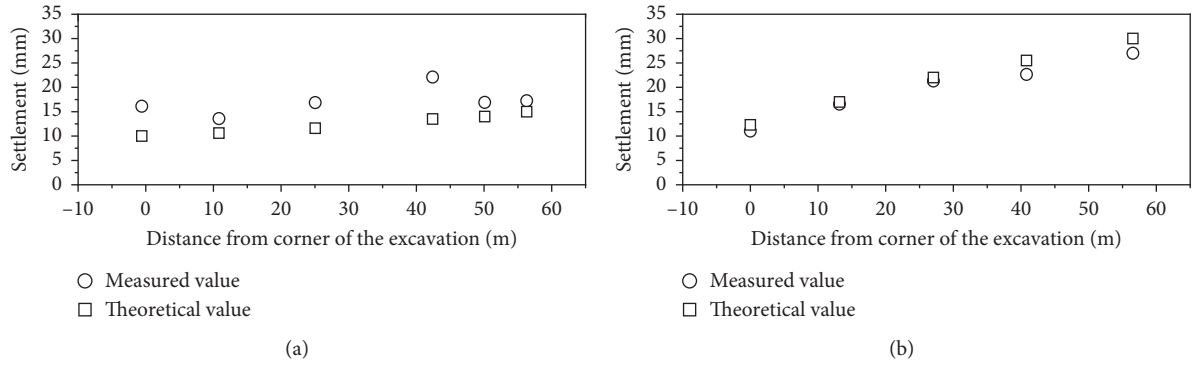

Figure 10: Comparison of theoretical and measured values of Fengqi Road excavation. (a) Side far from excavation. (b) Side near excavation.

values. In the case of Wulin Road, M32 is in the unaffected soil area, but it still exhibits subsidence. This is related to the integrity of the upper building, which biases the settlement value.

The frictional resistance and end resistance of the pile are changed because of the excavation. The calculation formula for the vertical bearing safety factor of a pile after excavation is as follows:

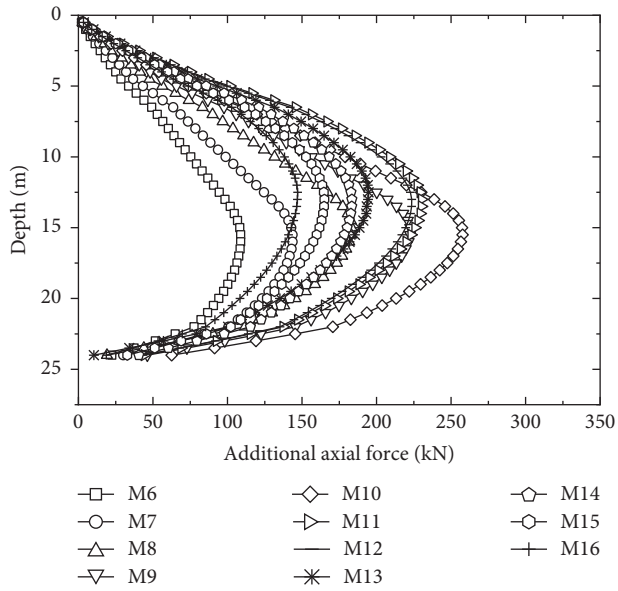

Figure 11: Additional axial force distribution of loaded pile of Fengqi road excavation.

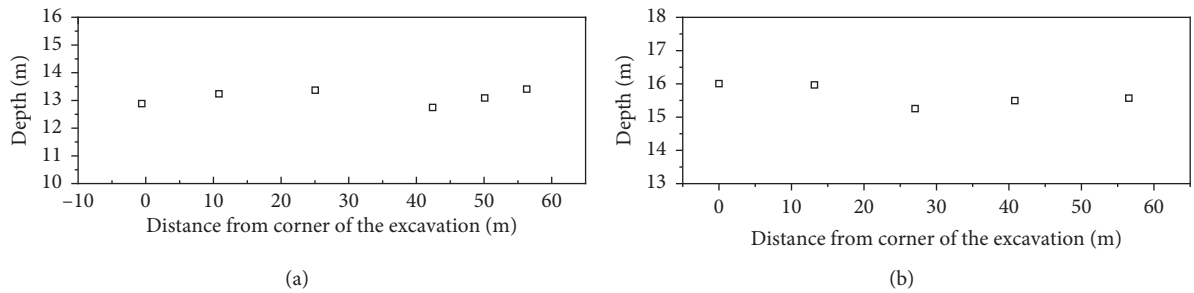

Figure 12: Depths of neutral points of Fengqi Road excavation. (a) Side far from excavation. (b) Side near excavation.

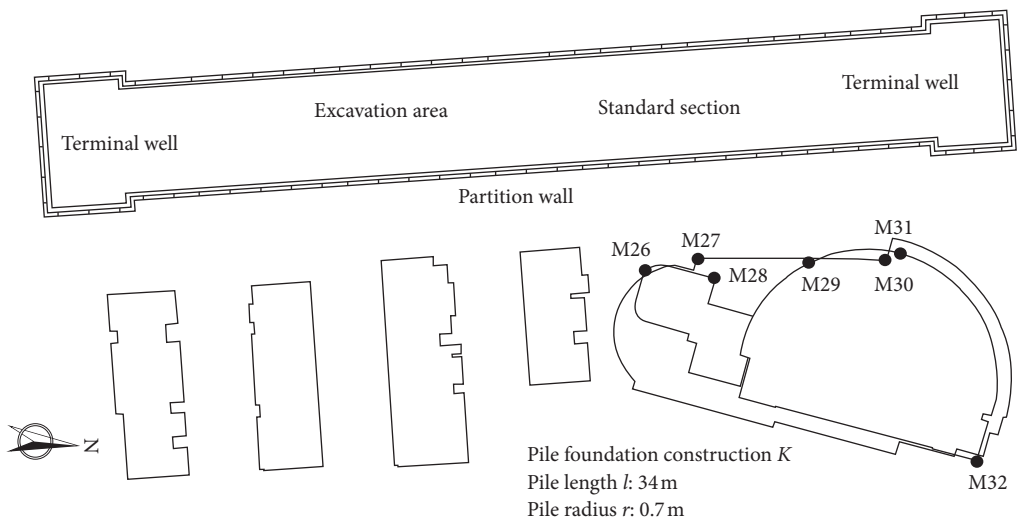

Figure 13: Plan of Wulin Road metro station and adjacent buildings. M26–M32 are the pile numbers.

Table 4: Soil profiles and parameters of Wulin Road excavation.

Layer number	Name of soil layer	h (m)	c (kPa)	φ (°)	E_s (MPa)	G_s (MPa)	I_P	I_L	ν	r_0 (m)	r_m (m)	δ (°)	R_{sf}
1	Fill	4	10	15	1.61	2.47	—	—					
2	Soft silty clay	7	13	9	2.3	3.54	16.0	1.13					
3	Soft silty clay or silt	5	14	11	2.8	4.31	11.9	1.3					
4	Soft silty clay	9	12	8.5	2.4	3.69	15.6	1.19	0.3	0.35	16.0	30	0.9
5	Soft clay	3	11	7.5	2.2	3.38	18.7	1.06					
6	Silty clay	6	23	13.5	3.5	5.38	16.4	0.74					
7	Sand	2	0	31	12	18.46	—	—					

Table 5: Observed soil surface settlements at measuring points of Wulin Road excavation.

Measuring points	M26	M27	M28	M29	M30	M31
Distance from corner	84	70.3	66.1	45.9	30	27
Observed settlement value (mm)	8.2	16.2	14.1	11.9	9.17	9.07

The northwest corner of the excavation serves as the reference point. Positive distance values indicate that the measuring point is located at the south side of the corner of excavation. The specific layout of the measurement points is shown in Figure 13.

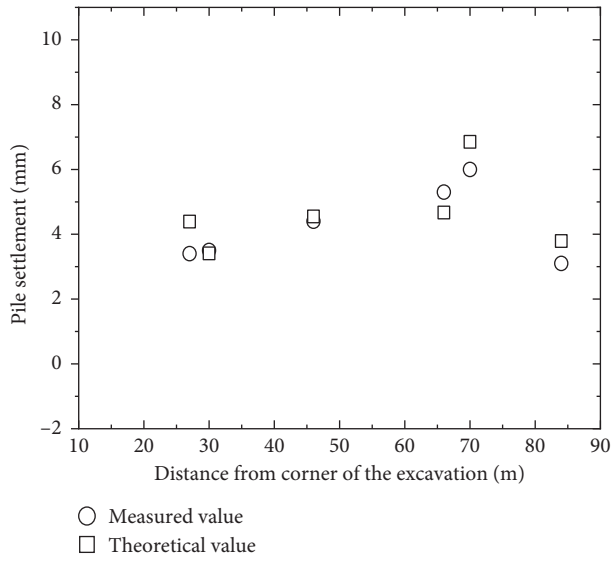

Figure 14: Comparison of theoretical and measured settlement values of Wulin Road excavation.

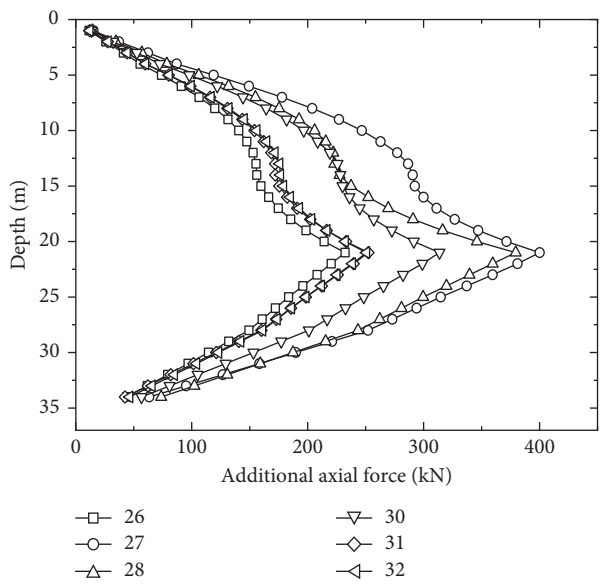

Figure 15: Additional axial force distribution of loaded pile of Wulin Road excavation.

$$K = \frac{Q_{uk}}{R_a} = \frac{\eta\left(\sum \tau_{bk} l_k u - \sum \tau_{bi} l_i u\right) + \xi p_{bm} A}{R_a}, \tag{13}$$

where Q_{uk} is the limiting value of bearing capacity, τ_{bk} is the positive frictional resistance caused by excavation, τ_{bi} is the negative frictional resistance caused by excavation, l is the length of microsegments, u is the perimeter of the pile, P_{bm} is the end resistance, A is the area of the pile, and η and ξ are coefficients. R_a is the value of the bearing capacity in design.

The limiting bearing capacity Q_{uk} of the single pile is reduced under negative friction, so during the excavation, the safety factor is decreased; in other words, the security is hampered. In the course of construction, the settlement of the building should be observed at all times, and protective measures should be taken when necessary.

7. Conclusions

A simplified theoretical method is proposed to predict the excavation-induced additional settlements of existing buildings. Two real cases are presented to verify this method, and the following conclusions were drawn:

(1) The regular behavior of excavation-induced soil settlements varies in two different areas. Near the excavation, the soil settlement first remains unchanged and then linearly decreases with increasing depth; in the area far from the excavation, the settlement linearly decreases. The boundary between the two areas is located at $1.0H_e$. A calculation formula for deep soil settlements is obtained in this study.

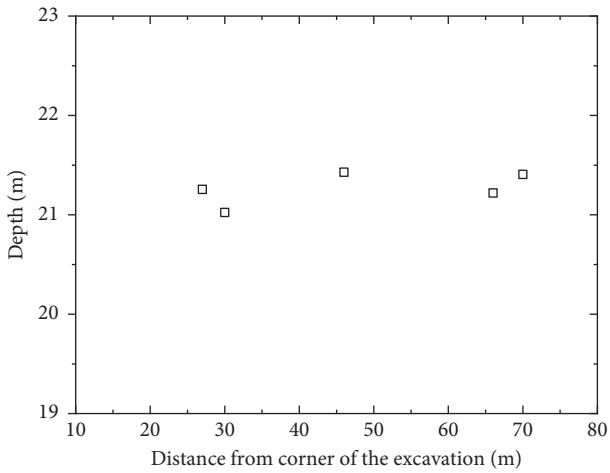

Figure 16: Depths of neutral points of Wulin Road excavation.

(2) The hyperbolic model with corrected parameters is proposed to calculate the positive skin friction, negative skin friction, and end resistance of existing piles induced by nearby excavation. The original points of the hyperbolic model are changed. The existing piles have already employed 50% of the limiting bearing capacity, based on the design code. The asymptotic value of the negative skin friction model is obtained with reference to the pile uplift. For the positive skin friction and end resistance, the value is increased to 120% because of the compression effect of soil.

(3) Comparison between the theoretical and measured values shows that the calculated values are in good agreement with the measured results. Near the excavation, the theoretical value is larger, but for distant points, the measured value is larger. This is related to the integrity of the upper building, which biases the settlement value.

The proposed simple calculation method is efficient and suitable to predict excavation-induced pile settlement. Although generally applicable, the influence of upper buildings has not been fully addressed. Therefore, the settlements of piles far from the excavation may be underestimated, particularly for piles located outside the affected soil area. This factor should be examined in further analyses.

Data Availability

The data used to support the findings of this study are included within the article.

Conflicts of Interest

There are no conflicts of interest regarding the publication of this paper.

Acknowledgments

This study was funded by the National Natural Science Foundation of China (No. 51608485), the 151 Talents Project of Zhejiang Province, the Zhejiang Provincial Natural Science Foundation (Nos. LQ18E090009 and LZ17E080002), and the Open Foundation of Engineering Research Center of Construction Technology of Precast Concrete of Zhejiang Province.

References

[1] A. L. Mana and G. W. Clough, "Prediction of movement for braced cuts in clay," *Journal of the Geotechnical Engineering Division*, vol. 107, pp. 759–777, 1981.

[2] G. W. Clough and T. D. O'Rourke, "Construction induced movements of in situ walls," *Proceedings of Design and Performance of Earth Retaining Structures, Geotechnical Special Publication No. 25*, pp. 439–470, ASCE, New York, USA, 1990.

[3] G. T. Kung, C. H. Juang, E. C. Hsiao, and Y. M. Hashash, "Simplified model for wall deflection and ground-surface settlement caused by braced excavation in clays," *Journal of Geotechnical and Geoenvironmental Engineering*, vol. 133, no. 6, pp. 731–747, 2007.

[4] L. Mu and M. Huang, "Small strain based method for predicting three-dimensional soil displacements induced by braced excavation," *Tunnelling and Underground Space Technology*, vol. 52, pp. 12–22, 2016.

[5] P.-G. Hsieh and C.-Y. Ou, "Shape of ground surface settlement profiles caused by excavation," *Canadian Geotechnical Journal*, vol. 35, no. 6, pp. 1004–1017, 1998.

[6] R. J. Finno, J. T. Blackburn, and J. F. Roboski, "Three-dimensional effects for supported excavations in clay," *Journal of Geotechnical and Geoenvironmental Engineering*, vol. 133, no. 1, pp. 30–36, 2007.

[7] J. Roboski and R. J. Finno, "Distributions of ground movements parallel to deep excavations in clay," *Canadian Geotechnical Journal*, vol. 43, no. 1, pp. 43–58, 2006.

[8] A. Contini, A. Cividini, and G. Gioda, "Numerical evaluation of the surface displacements due to soil grouting and to tunnel excavation," *International Journal of Geomechanics*, vol. 7, no. 3, pp. 217–226, 2007.

[9] E. E. Alonso, A. Josa, and A. Ledesma, "Negative skin friction on piles: a simplified analysis and prediction procedure," *Géotechnique*, vol. 34, no. 3, pp. 341–357, 1984.

[10] H. Kishida and M. Uesugi, "Tests of the interface between sand and steel in the simple shear apparatus," *Géotechnique*, vol. 37, no. 1, pp. 45–52, 1987.

[11] L.-Y. Xu, W.-D. Shao, Y.-Y. Xue, F. Cai, and Y.-Y. Li, "A simplified piecewise-hyperbolic softening model of skin friction for axially loaded piles," *Computers and Geotechnics*, vol. 108, pp. 7–16, 2019.

[12] W. Cao, Y. Chen, and W. E. Wolfe, "New load transfer hyperbolic model for pile-soil interface and negative skin friction on single piles embedded in soft soils," *International Journal of Geomechanics*, vol. 14, no. 1, pp. 92–100, 2014.

[13] Q.-Q. Zhang, L.-P. Li, and Y.-J. Chen, "Analysis of compression pile response using a softening model, a hyperbolic model of skin friction, and a bilinear model of end resistance," *Journal of Engineering Mechanics*, vol. 140, no. 1, pp. 102–111, 2014.

[14] Q.-Q. Zhang and Z.-M. Zhang, "A simplified nonlinear approach for single pile settlement analysis," *Canadian Geotechnical Journal*, vol. 49, no. 11, pp. 1256–1266, 2012.

[15] K. S. Wong and C. I. the, "Negative skin friction on piles in layered soil deposits," *International Journal of Rock Mechanics and Mining Sciences & Geomechanics Abstracts*, vol. 33, no. 3, pp. 457–465, 1996.

[16] H.-J. Kim and J. L. C. Mission, "Development of negative skin friction on single piles: uncoupled analysis based on nonlinear consolidation theory with finite strain and the load-transfer method," *Canadian Geotechnical Journal*, vol. 48, no. 6, pp. 905–914, 2011.

[17] K. T. Tran, M. McVay, R. Herrera, and P. Lai, "Estimation of nonlinear static skin friction on multiple pile segments using the measured hammer impact response at the top and bottom of the pile," *Computers and Geotechnics*, vol. 41, pp. 79–89, 2012.

[18] K. Cui, J. Feng, and C. Zhu, "A study on the mechanisms of interaction between deep foundation pits and the pile foundations of adjacent skewed arches as well as methods for deformation control," *Complexity*, vol. 2018, Article ID 6535123, 19 pages, 2018.

[19] N. Liu, N. Duan, and F. Yu, "Deformation characteristics of retaining structures and nearby buildings for different propped retaining walls in soft soil," *Journal of Testing and Evaluation*, vol. 47, no. 3, pp. 1829–1847, 2019.

[20] Q.-Q. Zhang, S.-W. Liu, R.-F. Feng, and X.-M. Li, "Analytical method for prediction of progressive deformation mechanism of existing piles due to excavation beneath a pile-supported building," *International Journal of Civil Engineering*, vol. 17, no. 6, pp. 751–763, 2019.

[21] A. T. C. Goh, K. S. Wong, C. I. Teh, D. Wen, and D. Wen, "Pile response adjacent to braced excavation," *Journal of Geotechnical and Geoenvironmental Engineering*, vol. 129, no. 4, pp. 383–386, 2003.

[22] F. Dezi, F. Gara, and D. Roia, "Linear and nonlinear dynamic response of piles in soft marine clay," *Journal of Geotechnical and Geoenvironmental Engineering*, vol. 143, no. 1, Article ID 04016085, 2017.

[23] Y. Zhou, A. Yao, H. Li, and X. Zheng, "Correction of earth pressure and analysis of deformation for double-row piles in foundation excavation in Changchun of China," *Advances in Materials Science and Engineering*, vol. 2016, Article ID 9818160, 10 pages, 2016.

[24] C.-Y. Ou, P.-G. Hsieh, and D.-C. Chiou, "Characteristics of ground surface settlement during excavation," *Canadian Geotechnical Journal*, vol. 30, no. 5, pp. 758–767, 1993.

[25] P. G. Hsieh and C. Y. Ou, "Shape of ground surface settlement profiles caused by excavation," *Comput Geotech*, vol. 38, no. 8, pp. 987–997, 2011.

[26] M. S. Caspe, "Surface settlement adjacent to braced open cuts," *Journal of the Soil Mechanics and Foundations Division*, vol. 92, no. 4, pp. 51–59, 1996.

[27] N. W. Liu, *Analysis of Plane and Spatial Deformation Characteristics of the Retaining Structure and Environmental Effects Assessment in Soft Soil*, Zhejiang University, Hangzhou, China, 2015.

[28] J. E. Gómez, G. M. Filz, and R. M. Ebeling, "Development of an improved numerical model for concrete-to-soil interfaces in soil-structure interaction analyses," Technical Report ITL-99-1, US Army Engineer Research and Development Center, Vicksburg, MS, USA, 2000.

[29] JGJ 94-2008, *Code for Design of Building Foundation*, China Architecture & Building Press, Beijing, China, 2008, in Chinese.

[30] J. D. Geddes, "Stresses in foundation soils due to vertical subsurface loading," *Géotechnique*, vol. 16, no. 3, pp. 231–255, 1966.

[31] K. M. Lee and Z. R. Xiao, "A simplified nonlinear approach for pile group settlement analysis in multilayered soils," *Canadian Geotechnical Journal*, vol. 38, no. 5, pp. 1063–1080, 2001.

[32] M. F. Randolph and C. P. Wroth, "An analysis of the vertical deformation of pile groups," *Géotechnique*, vol. 29, no. 4, pp. 423–439, 1979.

[33] Z. Zhang, Q. Zhang, and F. Yu, "A destructive field study on the behavior of piles under tension and compression," *Journal of Zhejiang University-SCIENCE A*, vol. 12, no. 4, pp. 291–300, 2011.

[34] Q. Q. Zhang, S. W. Liu, S. M. Zhang, J. Zhang, and K. Wang, "Simplified non-linear approaches for response of a single pile and pile groups considering progressive deformation of pile-soil system," *Soils and Foundations*, vol. 56, no. 3, pp. 473–484, 2016.

[35] V. G. Berezantve, V. Khristoforov, and V. Golubkvo, "Load bearing capacity and deformation of piled foundations," in *Proceedings of the 5th ICSMFE*, Paris, UK, 1961.